New Zealand 20th century sea level rise: Resolving the vertical land motion using space geodetic and geological data

Abdelali Fadil, Paul Denys, Robert Tenzer, Hugh R. Grenfell, Pascal Willis

JOURNAL OF GEOPHYSICAL RESEARCH: OCEANS, VOL. 118, 6076–6091, doi:10.1002/2013JC008867, 2013

New Zealand 20th century sea level rise: Resolving the vertical land motion using space geodetic and geological data

Abdelali Fadil,[1] Paul Denys,[1] Robert Tenzer,[2] Hugh R. Grenfell,[3] and Pascal Willis[4,5]

Received 20 February 2013; revised 14 October 2013; accepted 15 October 2013; published 15 November 2013.

[1] Investigations in long-term instrumental tidal records reveal that 20th century sea level along the coast of New Zealand is rising at 1.46 ± 0.10 mm/yr in agreement with the regional rates from southern Australia and Tasmania. We extend the advanced altimeter-gauge approach of combining satellite altimetry and tide gauge data with constraint equations from long-term adjacent tide gauge records to assess its performance in open seas and to explore the impact of vertical land motion on the observed relative sea level. This approach has again proven to be a robust method with an accuracy of 0.4 mm/yr. While no clear sea level rise pattern can be inferred once the tide gauge apparent sea level trends are corrected for vertical land motions from GPS, the advanced altimeter-gauge and geological vertical rates are completely consistent and reveal three temporal phases of sea level rise marked by an increase from 1.46 ± 0.10 mm/yr to 1.72 ± 0.10 mm/yr during the period (1900–1936), followed by a decrease to 1.48 ± 0.10 mm/yr during the period (1936–1956), and a substantial increase to 2.60 ± 0.10 mm/yr during the period (1956–1975). In contrast, the 20th century microfossil proxy records of absolute sea level rise display twice the tide gauge sea level rise rate of 3.17 ± 0.30 mm/yr and 3.28 ± 0.45 mm/yr, respectively, once salt-marsh records are corrected using GPS and geological vertical rates. Differential autocompaction and transfer functions are possible factors, which need further investigation.

Citation: Fadil, A., P. Denys, R. Tenzer, H. R. Grenfell, and P. Willis (2013), New Zealand 20th century sea level rise: Resolving the vertical land motion using space geodetic and geological data, *J. Geophys. Res. Oceans*, *118*, 6076–6091, doi:10.1002/2013JC008867.

1. Introduction

[2] Rising global sea levels are considered to be one of the consequences of global warming. Analysis of globally distributed sets of long-term tide gauge records indicates that sea level rose at an average rate of ∼1.7 ± 0.2 mm/yr during the 20th century with considerable variability in smaller regions of the oceans [e.g., *Holgate*, 2007; *Church and White*, 2011].

[3] New Zealand has been monitoring sea level since the 1890s and has some of the longest and most reliable tide gauge records in the southern hemisphere, which otherwise has only sparse data. The average relative sea level rise from the four long-term recording tide gauges at Auckland, Wellington, Lyttelton, and Dunedin is estimated at 1.80 ± 0.34 mm/yr during the 20th century (Figure 1 and Table 1) [*Hannah and Bell*, 2012]. Note that through this study unless otherwise specified the uncertainty on any computed average reflects the dispersion among the given trends, whereas uncertainty on each individual trend is one-sigma.

[4] Instrumental sea level data sets have a limited reach back in time and proxy indicators of sea level, such as foraminifera (microscopic, shelled protozoa), are useful to extend the record. Investigations in Tasmania and New Zealand [e.g., *Southall et al*., 2006; *Gehrels et al*., 2008, 2012; *Figueira*, 2012; *Grenfell et al*., 2012] have shown that study of salt-marsh sediments can produce valuable sea level records. The average relative sea level rise from these studies at sites located in the North and South Islands is evaluated at 3.15 ± 0.27 mm/yr over the 20th century (Table 1).

[5] Land uplift or subsidence that may occur at tide gauge and salt-marsh sites could be responsible for the spatial variability of the observed sea level trends (Table 1) and the difference of 1.35 mm/yr between the rates of proxy and instrumental sea level change. Glacial Isostatic Adjustment (GIA), present-day glacial ice melting [*Chinn et al*., 2005], active tectonics, volcanism, mantle dynamics, and anthropogenic causes (e.g., sedimentation, water pumping) are the

[1]National School of Surveying, University of Otago, Dunedin, New Zealand.
[2]Institute of Geodesy and Geophysics, School of Geodesy and Geomatics, Wuhan University, Wuhan, China.
[3]Geomarine Research, Auckland, New Zealand.
[4]Institut national de l'information géographique et forestière, direction technique, Saint-Mandé, France.
[5]Institut de Physique du Globe de Paris, Etudes Spatiales et Planetologie, Paris, France.

Corresponding author: A. Fadil, National School of Surveying, University of Otago, Box 56, Dunedin 9054, New Zealand. (abdelali.fadil@gmail.com)

2169-9275/13/10.1002/2013JC008867

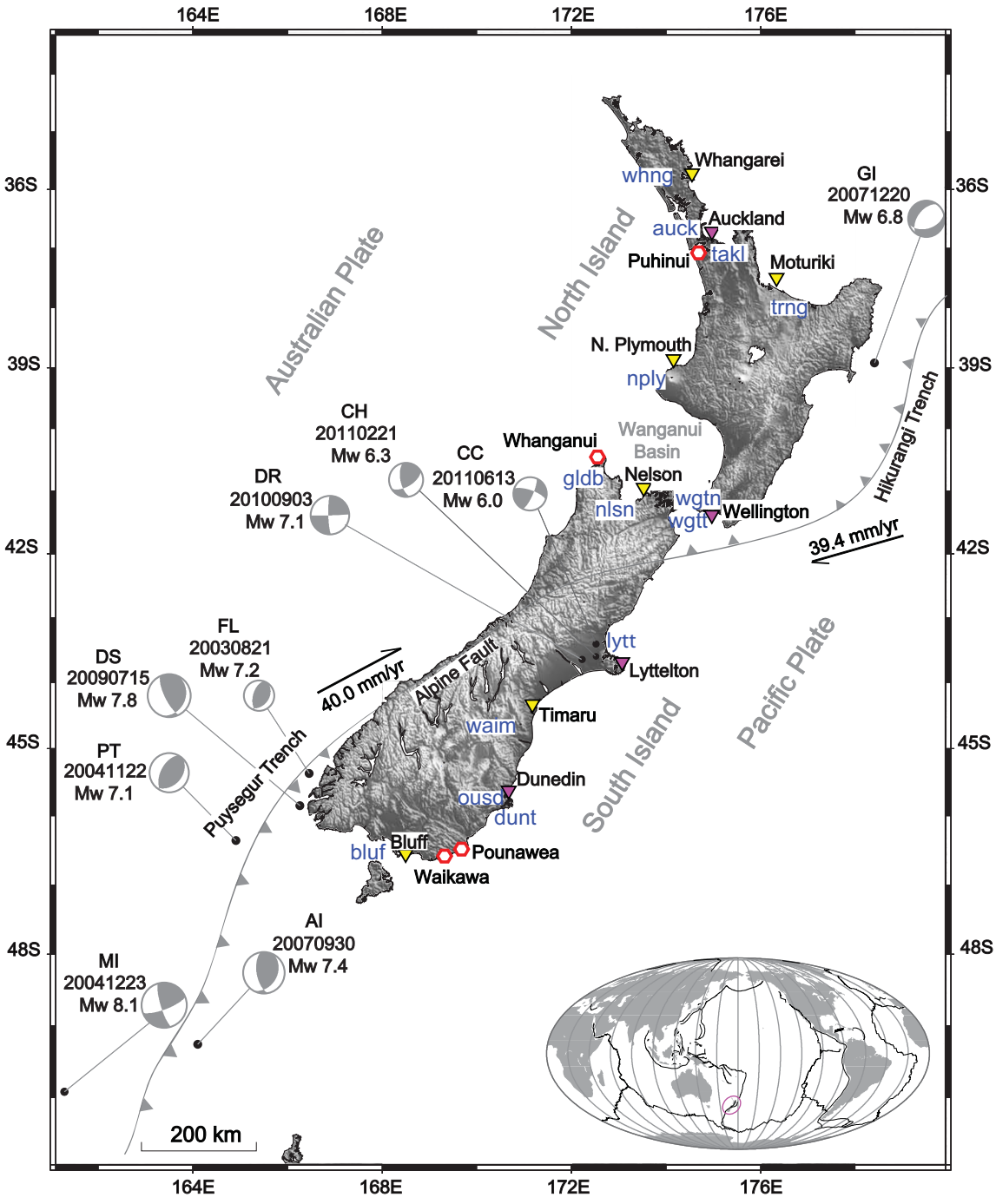

Figure 1. Geographic locations of New Zealand tide gauges with continuous recording (pink triangles) and with discontinuous recording (yellow triangles). Red hexagons represent locations of salt-marsh foraminiferal studies. cGPS stations nearby tide gauge and salt-marsh sites are shown by their four-character codes. Main regional tectonic setting of New Zealand is also shown. Fault traces are in gray: Hikurangi and Puysegur subduction trenches, and the Alpine fault. Black arrows show Pacific-Australia relative convergence from the MORVEL plate motion model [*DeMets et al*., 2010]. Moment tensors and magnitudes of the earthquakes that occurred during the 1996–present GPS record are taken from the Global Centroid Moment Tensor Catalogue and are indicated by two character codes: AI, Auckland Islands; CC, Christchurch; CH, Christchurch; DR, Darfield; DS, Dusky Sound; FL, Fiordland; GI, Gisborne; MI, Macquarie Island; and PT, Puysegur Trench. The inset shows the world map with major plate boundaries.

Table 1. New Zealand Relative Sea Level (RSL) Estimates From Tide Gauge (TG) and Salt-Marsh (SM) Records

							Period/TG RSL[b]	Period/TG RSL[c]	SM RSL[d]
Site	Lat.	Lon.	Data	Reference[a]	PSMSL	Gaps (%)	HB12 (mm/yr)	This Study (mm/yr)	FI12-GE08-GR12 (mm/yr)
Whangarei (1962–2011)	−35.76	174.35	TG	UHSLC	1065	40.8	(1962–2008)/2.20 ± 0.60	(1975–2011)/2.85 ± 0.55	
Auckland (1899–2011)	−36.85	174.76	TG	LINZ	150	2.7	(1899–2008)/1.70 ± 0.14	(1899–2011)/1.60 ± 0.25	
Puhinui (20th century)	−36.99	174.84	SM	GR12					3.00 ± 0.50
Moturiki (1949–2011)	−37.65	176.18	TG	NIWA	978	38.7	(1951–2008)/1.90 ± 0.20	(1974–2011)/1.80 ± 0.20	
New Plymouth (1920–2011)	−39.05	174.03	TG	LINZ	996	37.4	(1920–2008)/1.50 ± 0.20	(1920–2011)/1.50 ± 0.30	
Whanganui (20th century)	−40.58	172.61	SM	FI12					3.50 ± 0.50
Nelson (1939–2011)	−41.25	173.28	TG	PSMSL	787	70.8	(1941–2008)/1.30 ± 0.25	(1956–2011)/0.60 ± 0.25	
Wellington (1891–2011)	−41.28	174.78	TG	LINZ	221	6.7	(1901–2008)/2.20 ± 0.13	(1901–2011)/2.30 ± 0.15	
Lyttelton (1901–2011)	−43.60	172.71	TG	LINZ	247	13.7	(1901–2008)/2.00 ± 0.15	(1901–2011)/1.85 ± 0.15	
Timaru (1935–2011)	−44.40	171.26	TG	PSMSL	998	72.4	(1936–2008)/1.70 ± 0.25	(1963–2011)/2.20 ± 0.90	
Dunedin (1899–2011)	−45.88	170.51	TG	LINZ	136	17.0	(1899–2008)/1.30 ± 0.15	(1899–2011)/1.35 ± 0.15	
Pounawea (20th century)	−46.38	169.69	SM	GE08					2.80 ± 0.50
Waikawa (20th century)	−46.55	169.13	SM	FI12					3.30 ± 0.50
Bluff (1918–2011)	−46.60	168.35	TG	PSMSL	213	72.0	(1926–2008)/1.80 ± 0.15	(1923–2011)/1.90 ± 0.20	

[a]Annual mean relative sea level data are provided by the Land Information New Zealand (LINZ), the Permanent Service for Mean Sea Level (PSMSL), the National Institute of Water and Atmospheric Research (NIWA), and the University of Hawaii Sea Level Center (UHSLC). FI12, GE08, and GR12 denote the works of *Figueira* [2012], *Gehrels et al*. [2008], and *Grenfell et al*. [2012].
[b]The tide gauge RSL reference epochs and trends as given in *Hannah and Bell* [2012] abbreviated as HB12.
[c]The tide gauge RSL trends are estimated in this study from the available data sets shown in Figure 2.
[d]The salt-marsh RSL were estimated by *Gehrels et al*. [2008] at Pounawea, *Grenfell et al*. [2012] at Puhinui and *Figueira* [2012] at Whanganui Inlet and Waikawa.

most likely contributors to the vertical land motion [e.g., *Peltier*, 2004; *Argus et al*., 2005].

[6] The task of decoupling vertical land motion and sea level rise signals becomes more complicated and challenging for regions within a deforming plate boundary zone, such as the case of western Canada, the northwestern United States [e.g., *Mazzotti et al*., 2008], and New Zealand [e.g., *Walcott*, 1984]. The 1500 km section of the Pacific-Australian plate boundary through New Zealand includes segments of subduction, back-arc rifting, transform motion, and oblique continental collision (Figure 1).

[7] Over the last 17 years, substantial efforts have been undertaken to upgrade New Zealand's tide gauge network (Figure 1 and Table 1) with colocated continuous GPS stations (cGPS). With the advent of GPS global networks and data analysis, it has become both possible and realistic to estimate accurately vertical land motion at individual tide gauges [e.g., *Wöppelmann et al*., 2007].

[8] An alternative approach to computing vertical land motion was developed by *Mitchum* [1998] in order to monitor a low-frequency drift in sea surface height from satellite altimeters through the use of tide gauge sea level records. This classical altimeter-gauge principle consisted of differencing the tide gauge sea level time series with the equivalent satellite altimetry time series. An advanced altimeter-gauge algorithm adapted from the classical approach that includes supplementary equations from adjacent tide gauges with long-term records has been devised by *Kuo et al*. [2004, 2008], and applied in Fennoscandia, the Great Lakes, and Alaska. This approach has been extended by *Wöppelmann and Marcos* [2012] to investigate the contribution of the vertical land motions on the observed rates from 17 tide gauges along the coasts of southern Europe.

[9] This study provides contemporary constraints on New Zealand sea level rise by coupling instrumental and proxy sea level records with space geodetic and geological vertical land motion estimates. In section 2, relative sea level estimates from previous tide gauge and salt-marsh studies are reviewed and updated over the 20th century. Section 3 describes the GPS data analysis and the implementation of the advanced altimeter-gauge approach in New Zealand oceanic context. In section 4, space geodetic and geological vertical rate estimates are compared, and then combined with relative sea level trends to yield constraints on the rate of absolute sea level change around New Zealand over the 20th century.

2. Instrumental and Proxy Sea Level Records

2.1. Tide Gauge Relative Sea Level

[10] Although records from as many as 26 tide gauges are installed around New Zealand (http://www.psmsl.org/data/obtaining/nucat.dat) not all are considered suitable for this study. They are assessed according to two criteria: (1) tide gauge data span is required to cover at least two 18.6 yr nodal tides in order to retrieve accurate relative sea level trends and (2) to overlap with the satellite altimetry period for at least 8 years in order to determine stable vertical land motion from the classical altimeter-gauge approach [*Wöppelmann and Marcos*, 2012]. Ten tide gauges fulfilling this screening are listed in Table 1.

[11] The initial sea level trend analyses undertaken in New Zealand, as reported by *Hannah* [1990] and revised by *Hannah* [2004] only used sea level records from the four main continuously recording tide gauges located at Auckland, Wellington, Lyttelton, and Dunedin (Figure 2). These analyses were updated and extended by *Hannah and Bell* [2012] to include another six tide gauges located at Whangarei, Moturiki, New Plymouth, Nelson, Timaru, and Bluff (Figure 2), each with very discontinuous records. The

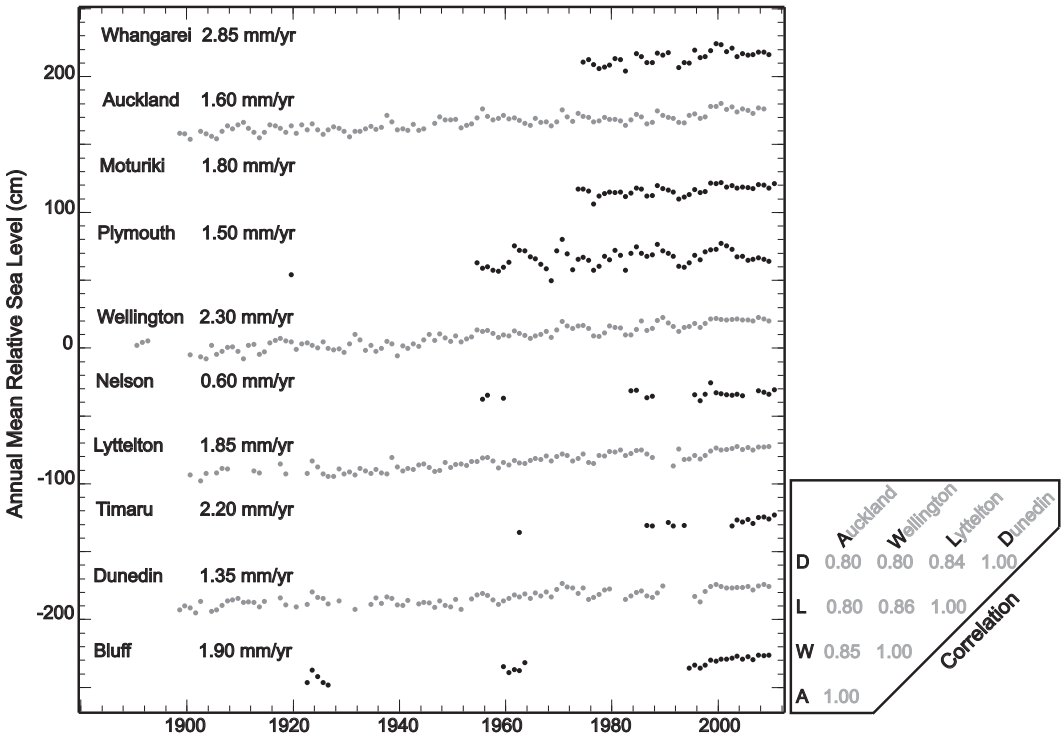

Figure 2. Annual mean relative sea level time series from New Zealand tide gauges with continuous (in gray) and discontinuous (in black) records. The associated relative sea level trends are shown at the top of each time series. Arbitrary offsets have been applied for clarity. The diagram shows relative correlation coefficients between pairs of tide gauges with long-term continuous sea level records. Bluff, Nelson, and Timaru data are retrieved from the Permanent Service for Mean Sea Level [*Woodworth and Player*, 2003]. Auckland, New Plymouth, Wellington, Lyttelton, and Dunedin data are from the Land Information New Zealand (LINZ). Moturiki data are from the National Institute of Water and Atmospheric Research (NIWA). Whangarei data are from the University of Hawaii Sea Level Center (UHSLC).

process followed to construct sea level at these six tide gauges involved (i) a comparison of the old mean sea level datum with a newly defined datum obtained from sea level records from the last decade and (ii) an assessment of the spatially coherent variability in annual sea level using an empirical orthogonal function analysis. The relative sea level trends calculated at these 10 tide gauges by *Hannah and Bell* [2012] are given in Table 1.

[12] Determinations of linear trends from time series with time-correlated noise using ordinary least-squares regression can underestimate the uncertainty on the rate parameter significantly [e.g., *Langbein and Johnson*, 1997; *Mao et al*., 1999]. Using a maximum likelihood estimation technique implemented in CATS software [*Williams*, 2008], new relative sea level trends with realistic uncertainties are computed in this study (Table 1) from the available annual sea level data sets (Figure 2) archived at the Land Information New Zealand (LINZ), the National Institute of Water and Atmospheric Research (NIWA), the Permanent Service for Mean Sea Level (PSMSL) [*Woodworth and Player*, 2003], and the University of Hawaii Sea Level Center (UHSLC). Auckland, Bluff, Dunedin, Lyttelton, New Plymouth, and Wellington sea level time series are best described by a combined power-law plus white noise model, whereas Nelson, Moturiki, Timaru, and Whangarei time series are best fitted by a combined first-order Gauss-Markov plus white noise model [e.g., *Williams*, 2008; *Langbein*, 2012].

2.2. Salt-Marsh Relative Sea Level

[13] In an attempt to provide further insight into sea level change in such data sparse regions, various studies have investigated the salt-marsh foraminiferal sea level records. Salt-marshes are located in the upper part of the intertidal zone (roughly between mean high and extreme high water spring) where sediments accumulate during flooding by the highest tides. Thick salt-marsh sediment accumulations may form when accommodation space is created by rising sea level [e.g., *Scott et al*., 2001; *Gehrels et al*., 2005].

[14] The distribution of high-tidal salt-marsh foraminifera with respect to elevation and local tidal conditions has been studied globally [e.g., *Hayward et al*., 1999; *Scott et al*., 2001; *Gehrels et al*., 2005; *Massey et al*., 2006]. With their narrowly defined vertical zones relative to sea level, salt-marsh foraminifera can be used to estimate former sea levels to an accuracy of about ± 5 cm [*Southall et al*., 2006]. The reconstruction of past sea levels makes use of transfer functions and a modern analogue technique to provide a history of sea level rise by relating the fossil assemblages to assemblages found in modern training sets.

This methodology has been extensively used in the northern hemisphere by several authors [e.g., *Edwards et al*., 2004; *Gehrels et al*., 2005; *Massey et al*., 2006; *Leorri et al*., 2008; *Kemp et al*., 2009]. The results derived from transfer functions should be treated with caution as they can obviously contribute significant errors. Publications should provide online access to their raw data and details of the transfer function calculations used if validation is thought necessary.

[15] *Southall et al*. [2006] first demonstrated that New Zealand salt-marsh foraminiferal faunas are an important tool for local sea level reconstructions. *Gehrels et al*. [2008] showed that sea level at Pounawea in the Catlins (Figure 1) was slowly rising at 0.5 ± 0.4 mm/yr before 1900, but during the 20th century increased substantially to 2.8 ± 0.5 mm/yr (Table 1).

[16] To better understand the New Zealand record of sea level rise over the last 700 years further sequences at Puhinui (northern North Island, *Grenfell et al*. [2012]), Whanganui Inlet, and Waikawa Harbour (north-western and south-eastern South Island, respectively, *Figueira* [2012]) have been cored and their foraminiferal faunas analyzed (Figure 1). The constructed sea level curves for the three sites indicate that sea level rose ~0.5–0.6 m over the past ~600 years (a similar rate to Pounawea), and appears to have accelerated in the late 19th to early 20th century with rates of about 3.0 ± 0.5 mm/yr over the 20th century (Table 1).

[17] All these foraminiferal studies have targeted sites as tectonically stable as possible with minimal depth to a non-compacting basement where possible. However, the effect of possible autocompaction [e.g., *Brain et al*., 2011, 2012], which could increase the reported foraminiferal proxy sea level rise rates, has not been fully accounted for. *Brain et al*. [2012] state that dry or bulk density core data provide only a limited insight into potential compaction effects and that new data is required to fully understand compaction processes, including creep and biodegradation. However, the general agreement of rates in the upper part of these cores (where there is minimal or no compaction) with rates derived from satellite altimetry data (for the last 20 years) provides some confidence in the proxy data.

[18] Monitoring the vertical land motion at the coast constitutes a key step toward correctly comparing the sea level rise from tide gauges and salt-marshes and thus identifying the relative contributions due to climate change [e.g., melting of land-based ice, ocean thermal expansion].

3. Data Sets Analysis

3.1. GPS Data Analysis

[19] Each of the investigated tide gauge and salt-marsh sites are located in the vicinity of one or two cGPS stations (Figure 1 and Table 1), for which raw data are publicly available from the New Zealand GeoNet archive (http://geonet.org.nz) and span from 7 to 17 years (Figure 3). An uniform analysis of GPS data is carried out in a consistent way all over the considered data period (1996–2012) with respect to the precise point positioning (PPP) mode implemented in the GIPSY-OASIS II 6.1.2 software package [*Webb and Zumberge*, 1995; *Zumberge et al*., 1997] using the single receiver phase ambiguity resolution algorithm [*Bertiger et al*., 2010] and the JPL reprocessed products as at 2012 (ftp://sideshow.jpl.nasa.gov/pub/JPL_GPS_Products/Final).

[20] The Vienna mapping function [*Boehm et al*., 2006] and nominal zenith hydrostatic delay based on the European Centre for Medium-Range Weather Forecasts data [*Tregoning and Herring*, 2006] are applied, while the zenith wet delay and the horizontal tropospheric gradients (north and east) are modeled as random walk variables, and estimated every 5 min as time-dependent parameters [*Bar-Sever et al*., 1998]. Solid earth and pole tide corrections following the IERS Conventions 2010 [*IERS Conventions*, 2010], ocean loading corrections using the FES2004 ocean tide model [*Lyard et al*., 2006], antenna phase center models [*Schmid et al*., 2007], diurnal and semidiurnal tidal atmospheric loading displacements [*Ponte and Ray*, 2002; *Tregoning and Watson*, 2009, 2011], and nontidal atmospheric loading corrections are taken into account [*Tregoning and Watson*, 2009].

[21] The resulting daily solutions are aligned to the ITRF2008 reference frame [*Altamimi et al*., 2011] using a seven-parameter Helmert transformation, and cleaned of outliers and discontinuities [*Herring*, 2003] that may be due to antenna changes and/or earthquakes and/or slow slip events (SSE) [e.g., *Wallace and Beavan*, 2010; *Wallace et al*., 2012] (Figure 3).

[22] Previous works [e.g., *Langbein and Johnson*, 1997; *Mao et al*., 1999] demonstrated that the measurement noise associated with the detrended GPS position time series residuals is time-correlated. Therefore, the formal errors on the GPS derived velocities are roughly underestimated by a factor of 5–10 if correlations are not properly accounted for. To assign realistic uncertainties to the GPS derived vertical velocities (Table 2), we carefully examined the GPS vertical time series using CATS software [*Williams*, 2008] that simultaneously estimates linear trends, annual and semiannual signal terms, power-law and time-variable white noise parameters, and offsets at specified times. A combination of power-law plus time-variable white noise model provides the most likely stochastic description of the GPS vertical time series, which is consistent with former studies [e.g., *Mao et al*., 1999]. The average spectral index is -0.85 ± 0.15, which is close to -1, indicating flicker noise [e.g., *Williams*, 2008; *Langbein*, 2012].

3.2. Combining Satellite Altimetry and Tide Gauge Records

3.2.1. Classical Altimeter-Gauge Approach

[23] Global ($1/4° \times 1/4°$) gridded altimetric sea level arrays (known as Delayed Time Mean Sea Level Anomalies "Reference Mission" products (DT MSLA REF TP/J1/J2) are compiled by the Archiving, Validation, and Interpretation of Satellite Oceanographic (AVISO) data center. This data set is produced by combining records from TOPEX/Poseidon, Jason-1, and Jason-2 satellites, which have monitored the same ground track since October 1992. The stability of the terrestrial reference frame realized by the TOPEX and Jason orbit has been carefully investigated and that all mean sea level results are provided in the ITRF2008 reference frame [*Lemoine et al*., 2010]. All the state-of-the-art geophysical corrections are applied to this data set: solid earth, ocean and pole tides, wet and dry

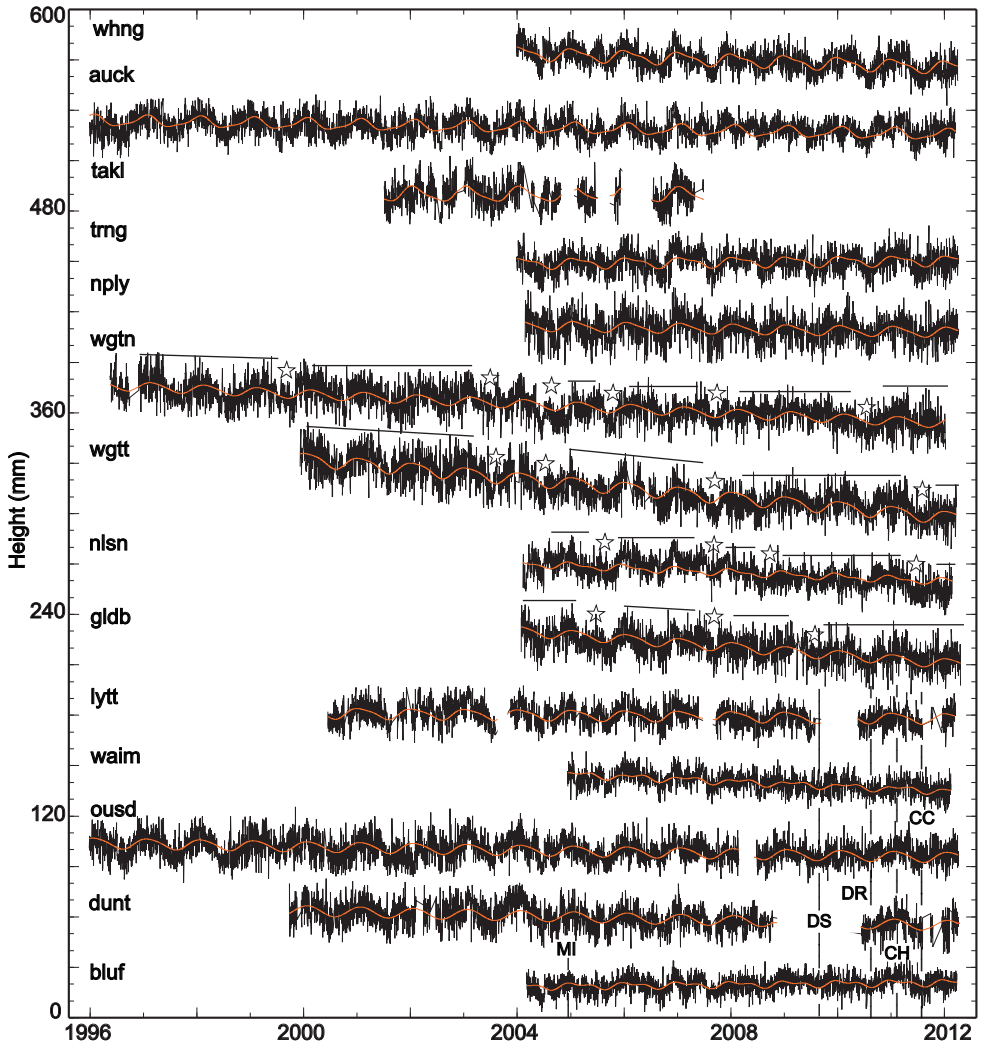

Figure 3. GPS vertical time series relative to the ITRF2008 reference frame. Arbitrary offsets have been applied for clarity. The orange line on each time series represents a linear model that incorporates annual and semiannual periodic signals. The black vertical dashed lines represent the epochs of the earthquakes that caused significant displacement. CC, CH, DR, DS, and MI earthquakes are shown in Figure 1. Slow slip events (black stars) have been recorded at cGPS stations (gldb, nlsn, wgtn, and wgtt) around the Wanganui basin (Figure 1).

troposphere, ionosphere, and inverted barometer. Since AVISO data are interpolated altimetry fields, the satellite altimetry time series associated with each tide gauge are built from its closest grid point. An average of the closest grid points to each tide gauge within a radius of 1/2° is also considered and discussed in section 4.2.

[24] The monthly averaged tide gauge data are obtained from LINZ, UHSLC, and NIWA (Figure 4). We applied an atmospheric correction to these data using the AVISO dynamic atmospheric corrections products [*Volkov et al*., 2007] that are already applied to the altimetry data. These products combine correction of the ocean response to atmospheric wind and pressure forcing, which is computed using Mog2D barotropic model [*Carrere and Lyard*, 2003] for high frequencies (<20 days), and an inverted barometer correction for lower frequencies.

[25] Given the absolute (geocentric) sea level g_i provided by the satellite altimetry at a tide gauge site i, it is possible to estimate the rate of the vertical land motion u_i at the benchmark to which this tide gauge is referenced by:

$$u_i = g_i - S_i^{Alt} \tag{1}$$

where S_i^{Alt} is the relative sea level change as measured by this tide gauge for the altimetry data period. There is an inherent assumption that the drifts associated with altimeter and tide gauge, which are inseparable from u_i, are small and negligible [*Kuo et al*., 2004].

[26] Finally, the vertical land motion estimate u_i and realistic uncertainty σu_i (Table 2) are computed from the altimeter-gauge sea level time series using CATS software [*Williams*, 2008]. A combined first-order Gauss-Markov plus white noise model provides the most likely stochastic description of the altimeter-gauge time series.

Table 2. Vertical Land Motions at the Tide Gauge and Salt-Marsh Sites From Geology, GPS, Classical (ALT-TG^{CLS}) and Advanced (ALT-TG^{ADV}) Altimeter-Gauge Approaches, and GIA[a]

				GPS			ALT-TG			
Site	cGPS	Dist[b] (km)	Geol.[c] (mm/yr)	ULR5[d] (mm/yr)	NZ3P[e] (mm/yr)	MVLM[f] (mm/yr)	ALT-TG^{OST} (mm/yr)	ALT-TG^{CLS} (mm/yr)	ALT-TG^{ADV} (mm/yr)	GIA[g] (mm/yr)
Whangarei	WHNG	16.0	~0 (0.0 ± 0.5)		−1.04 ± 0.57	−1.04 ± 0.57	2.77	0.20 ± 1.00	−0.38 ± 0.61	−0.06
	AUCK	27.0		−0.22 ± 0.15	−0.52 ± 0.33					
Auckland			~0 (0.0 ± 0.5)			−0.26 ± 0.21	−1.33	−0.70 ± 0.70	−0.16 ± 0.31	0.03
	TAKL	CLC		−0.21 ± 0.27	−0.07 ± 0.70					
Puhinui	TAKL	18.0	~0 (0.0 ± 0.5)	−0.21 ± 0.27	−0.07 ± 0.70	−0.14 ± 0.38				0.03
Moturiki	TRNG	10.0	0–1 (0.5 ± 0.5)		0.19 ± 0.45	0.19 ± 0.45	–	0.75 ± 0.50	0.59 ± 0.50	0.09
New Plymouth	NPLY	16.0	0–1 (0.5 ± 0.5)		−0.47 ± 0.28	−0.47 ± 0.28	8.29	4.28 ± 0.56	–	0.05
Whanganui	GLDB	27.0	0–1 (0.5 ± 0.5)		−2.40 ± 0.30	−2.40 ± 0.30				0.00
Nelson	NLSN	15.0	~0 (0.0 ± 0.5)		−1.31 ± 0.60	−1.31 ± 0.60	0.46	0.60 ± 1.10	0.68 ± 0.53	0.03
	WGTN	5.0		−2.31 ± 0.24	−1.74 ± 0.26					
Wellington			−1–0 (−0.5 ± 0.5)			−2.44 ± 0.13	−0.25	0.05 ± 0.40	−0.92 ± 0.30	0.03
	WGTT	0.5		−2.83 ± 0.33	−2.86 ± 0.21					
Lyttelton	LYTT	CLC	−1–0 (−0.5 ± 0.5)	−1.53 ± 0.20[h]	−0.28 ± 0.30 (−0.30 ± 0.34)[i]	−0.28 ± 0.30	−3.17	−1.15 ± 0.35	−0.44 ± 0.30	0.02
Timaru	WAIM	39.0	~0 (0.0 ± 0.5)		−1.40 ± 0.40 (−1.07 ± 0.53)[i]	−1.40 ± 0.40	–	−2.30 ± 1.20	−0.05 ± 0.69	0.07
	OUSD	11.0		−0.57 ± 0.18	−0.52 ± 0.30 (−0.56 ± 0.32)[i]					
Dunedin			~0 (0.0 ± 0.5)			−0.69 ± 0.12	0.35	0.00 ± 0.70	0.16 ± 0.33	−0.02
	DUNT	0.4		−0.94 ± 0.20	−0.72 ± 0.29 (−0.70 ± 0.33)[i]					
Pounawea	BLUF	109.0	~0 (0.0 ± 0.5)		0.28 ± 0.38 (0.51 ± 0.36)[j]	0.28 ± 0.38				−0.08
Waikawa	BLUF	64.0	~0 (0.0 ± 0.5)		0.28 ± 0.38 (0.51 ± 0.36)[j]	0.28 ± 0.38				−0.08
Bluff	BLUF	4.0	~0 (0.0 ± 0.5)		0.28 ± 0.38 (0.51 ± 0.36)[j]	0.28 ± 0.38	2.40	1.70 ± 0.50	−0.33 ± 0.33	−0.08

[a]Vertical land motions as computed without uncertainties by *Ostanciaux et al*. [2012] using classical altimeter-gauge approach is referred to as ALT-TG^{OST}.
[b]Dist indicates approximate distance between tide gauge or salt-marsh site and nearest cGPS. CLC stands for colocated.
[c]Geological vertical rates as compiled in *Beavan and Litchfield* [2012] and references therein.
[d]ULR5 solution is made available by *Santamaria-Gomez et al*. [2012] at http://www.sonel.org/IMG/txt/ulr5_vertical_velocities_table.txt.
[e]NZ3P stands for our New Zealand GPS data analysis described in section 3.1.
[f]MVLM stands for mean vertical land motion of ULR5 and NZ3P estimates. Assuming zero correlations, the associated uncertainty is the mean of the square root of the sum of the squares of the formal errors.
[g]Vertical land motion predictions from GIA ICE-5G (v1.3, VM2, L90) model tabulated at all PSMSL tide gauges and made available by *Peltier* [2004] at: http://www.atmosp.physics.utoronto.ca/~peltier/data sets/psmsl/drad250.PSMSL.ICE5Gv1.3_VM2_L90_2012b.txt.
[h]A close examination into ULR5 GPS vertical time series (available at http://www.sonel.org/-Solutions-.html) clearly shows that the discrepancy between ULR5 and NZ3P vertical rate estimates at LYTT is due to an offset that is not properly accounted for in ULR5 solution. ULR5 estimate at LYTT has been then disregarded.
[i]Vertical land motion estimates from the resultant time series of cGPS stations at LYTT, WAIM, OUSD, and DUNT using a combined time-variable white and power-law noise model with the CATS software [*Williams*, 2008] for the period up to 2009 Dusky Sound earthquake, and for the period between 2004 Macquarie Island and 2009 Dusky Sound earthquakes (Figures 1 and 3).
[j]Vertical land motion estimates from the resultant time series of cGPS stations at BLUF using a combined time-variable white and power-law noise model with the CATS software [*Williams*, 2008] for the period between 2004 Macquarie Island and 2009 Dusky Sound earthquakes (Figures 1 and 3).

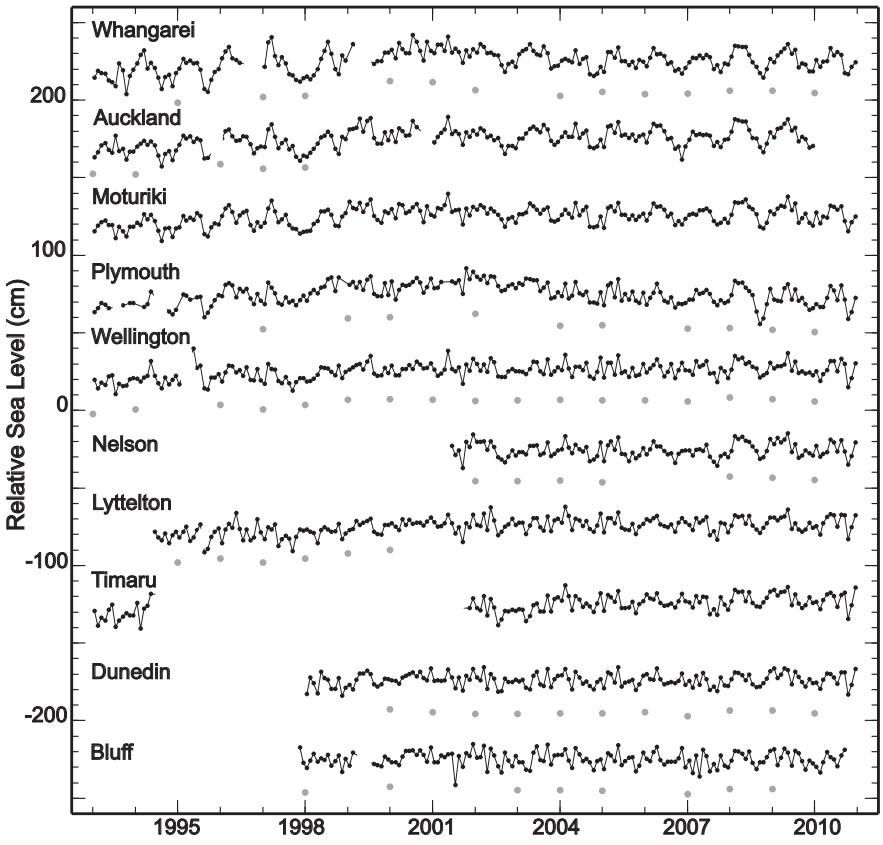

Figure 4. Monthly mean relative sea level (in black) used in this study at Whangarei (UHSLC), Auckland (LINZ), Moturiki (NIWA), New Plymouth (UHSLC), Wellington (LINZ), Nelson (UHSLC), Lyttelton (LINZ), Timaru (UHSLC), Dunedin (LINZ), and Bluff (UHSLC). Annual mean relative sea level (in gray) as retrieved from PSMSL archive and used by *Ostanciaux et al*. [2012] to estimate vertical land motion rates at New Zealand tide gauges using the classical altimeter-gauge approach. Arbitrary offsets have been applied for clarity.

3.2.2. Advanced Altimeter-Gauge Approach

[27] The current time span of satellite altimetry data is too short (~20 years) to derive an accurate trend from the altimeter-gauge time series that are strongly affected by interannual and decadal sea level signals and notably by the 18.6 year nodal tide [*Trupin and Wahr*, 1990], which leads to uncertainties of the order of 1–2 mm/yr depending on the length of the altimeter-gauge time series and the tide gauge latitude [e.g., *Ray et al*., 2010; *Woodworth*, 2012].

[28] The advanced altimeter-gauge approach, originally developed and applied by *Kuo et al*. [2004], is particularly valid in lakes and semienclosed seas where all tide gauge records display coherent long-term absolute sea level variations. To take advantage of any available historic tide gauge records and therefore reducing the solution uncertainty, *Kuo et al*. [2004] introduced the relative vertical land motion ru_{ij} between two nearby tide gauge sites i and j, assuming that both tide gauges measure an identical absolute sea level signal:

$$ru_{ij} = u_i - u_j = S_{j-i}^{TG} \tag{2}$$

where S_{j-i}^{TG} and σru_{ij} are the trend and uncertainty of the differenced sea level time series between the pair of tide gauges sites i and j computed using a combined first-order Gauss-Markov plus white noise model within CATS software [*Williams*, 2008].

[29] Under this assumption, the advanced altimeter-gauge approach has been extended by *Wöppelmann and Marcos* [2012] to the Mediterranean Sea as a semienclosed sea. The set of constraints is based on the observed correlations (of at least 0.6) and overlapping periods (to be at least 30 years) between the pairs of tide gauges (equation (2)). In this study, we attempt to explore this novel approach in the open oceans since New Zealand straddles the Tasman Sea and Pacific Ocean with long-term tide gauge sea level time series of up to 110 years at Auckland, Wellington, Lyttelton, and Dunedin exhibiting strong correlations with relative coefficients higher than 0.8 (Figure 2). For completeness, the solution algorithm adopted by *Wöppelmann and Marcos* [2012] is recalled and applied here.

[30] Equations (1) and (2) applied to n tide gauge sites can be expressed in the following vector-matrix notation:

$$\begin{bmatrix} I \\ F \end{bmatrix} m = \begin{bmatrix} d \\ h \end{bmatrix} \tag{3}$$

where I is the identity matrix of order n, m is the vector of unknowns, d is the observation vector, F is a $p \times n$ matrix

with p being the number of constraint equations representing the pairs of tide gauges considered and h their vector of relative vertical land motions. The vectors m and d are given by

$$m=\begin{pmatrix} u_1 \\ u_2 \\ \dots \\ u_{n-1} \\ u_n \end{pmatrix} \text{ and } d=\begin{pmatrix} g_1 - S_1{}^{Alt} \\ g_2 - S_2{}^{Alt} \\ \dots \\ g_{n-1} - S_{n-1}{}^{Alt} \\ g_n - S_n{}^{Alt} \end{pmatrix}$$

[31] The constraint equations are formed from pairs of adjacent tide gauges from the North Island, Cook Strait, and South Island according to the following scheme:

$$Pairs \begin{pmatrix} North\ Island & (Whangarei-Auckland-Moturiki) \\ Cook\ Strait & (Plymouth-Wellington-Nelson) \\ South\ Island & (Timaru-Lyttelton-Dunedin-Bluff) \\ Link & (Auckland-Wellington-Lyttelton \\ & \quad -Dunedin) \end{pmatrix} \tag{4}$$

[32] Pairs from any two tide gauges with discontinuous records are not included as the overlapping period will not contain sufficient common data to derive an accurate relative vertical land motion trend. Constraint equations involving Auckland, Wellington, Lyttelton, and Dunedin are introduced to link the three regions. Separate treatment of the three regions is also considered and will be discussed later.

[33] The system of observation equations (3) can be solved using the method of Lagrange multipliers [*Menke*, 2012] as follows:

$$\begin{bmatrix} I & F^T \\ F & 0 \end{bmatrix} \begin{bmatrix} m \\ \lambda \end{bmatrix} = \begin{bmatrix} d \\ h \end{bmatrix} \tag{5}$$

[34] Equation (5) is a linear system of the form $A \cdot x = Y$ whose simple least squares solution is given by

$$x=(A^TA)^{-1}(A^TY) \tag{6}$$

where the first n elements of x correspond to the vector of unknowns m while the other p elements are the Lagrange multipliers. According to the general least squares theory, the uncertainties of the vector m can be estimated from the diagonal terms of the associated covariance matrix $(A^TWA)^{-1}$, where the weight matrix W is defined as

$$W=diag\begin{bmatrix} \sigma u^2 \\ \sigma ru^2 \end{bmatrix}^{-1} \tag{7}$$

4. Results and Discussion

[35] Table 2 provides vertical land motion estimates at the investigated tide gauge and salt-marsh sites using GPS and altimeter-gauge approaches. Long-term geological rates of New Zealand coastline, as compiled by *Beavan and Litchfield* [2012] from 125 ka marine geological markers, are also reported (column 4). The predictions from *Peltier* [2004] GIA model given in the last column show rates $< \pm 0.1$ mm/yr suggesting that tectonic motion may be the dominant factor in any vertical land motion. The current rates of tectonic motions estimated from geological markers over 125 ka are thus not affected significantly by the late-Pleistocene ice melting occurring since 20 ka. It is, however, important to note that ICE-5G ice sheet history [*Peltier*, 2004] does not include New Zealand. The regional effect of the ice melting is thus unknown. Moreover, the influence of the present-day glacier melting in New Zealand on the VLM is not yet documented in literature. It should also be noted that *King et al*. [2012] compare modeled GIA uplift with vertical land motions at ~300 cGPS stations located near a global set of tide gauges, and find regionally coherent differences of commonly ± (0.5–2) mm/yr. The authors suggest that deficiencies in the ice history are the most likely source of these discrepancies.

4.1. GPS Vertical Land Motion Estimates

[36] For comparison and combination, GPS vertical land motion estimates, where available from the latest reanalyzed ITRF2008 solution of ULR consortium [*Santamaria-Gomez et al*., 2012], are reported (column 5 in Table 2). Our solution, NZ3P, is in good agreement with ULR5 with a mean difference of 0.11 ± 0.26 mm/yr. Inspection into the ULR5 time series of cGPS station at LYTT shows that the difference between the two solutions is related to an offset that was not properly accounted for in the ULR5 solution. Reestimation of the offsets from the ULR5 residual time series of LYTT station reveals that one of the offsets is significant at a two-sigma level. Although our GPS time series are 2 years longer than the ULR5 time series, our solution shows higher uncertainties. Note that for the ULR5 solution, the offsets affecting the GPS time series are not computed within CATS software, but removed beforehand. A recalculation of the ULR5 trends, uncertainties, and offsets within the CATS software shows higher uncertainties than those derived from our solution. The mean of the two solutions computed for the tide gauge and salt-marsh sites (column 7) will be used later to correct their relative sea level trends.

[37] During the period of the GPS record (1996–2012), there have been nine large earthquakes in the vicinity of New Zealand coastline (Figure 1): Fiordland (M_w 7.2, 20030821), Puysegur Trench (M_w 7.1, 20041122), Macquarie Island (M_w 8.1, 20041223), Auckland Islands (M_w 7.4, 20070930), Gisborne (M_w 6.8, 20071220), Dusky Sound (M_w 7.8, 20090715), Darfield (M_w 7.1, 20100903), and Christchurch (M_w 6.3, 20110221 and M_w 6.0, 20110630).

[38] Five of these events (Macquarie Island, Dusky Sound, Darfield, and Christchurch earthquakes) caused significant coseismic vertical displacements at 5 of the 14 investigated cGPS stations (LYTT, WAIM, DUNT, OUSD, and BLUF) located south-eastern South Island (Figure 3). Although two of these events (Macquarie Island and Dusky Sound) generate clear postseismic horizontal deformations

at cGPS stations of WAIM (Dusky Sound), BLUF (Macquarie Island and Dusky Sound), and OUSD (Dusky Sound), no observable postseismic deformation has been recorded across the vertical component of these cGPS stations (Figure 3).

[39] Preseismic vertical land motion rates are derived, using a combined time-variable white and power-law noise model within the CATS software [*Williams*, 2008], prior to Dusky Sound earthquake (Figure 3) at cGPS stations of LYTT, WAIM, DUNT, and OUSD, and between Macquarie Island and Dusky Sound earthquakes at cGPS station of BLUF. The estimated preseismic and long-term rates are consistent with a maximum difference of 0.3 mm/yr at cGPS station of WAIM (column 6 in Table 2).

4.2. Altimeter-Gauge Vertical Land Motion Estimates

[40] In order to identify global or regional vertical land motion trends, *Ostanciaux et al*. [2012] applied the classical altimeter-gauge approach at 634 globally distributed tide gauges by combining their annual mean sea level records and AVISO satellite altimetry. For comparative purposes, the vertical land motion estimates where available from this data set as published without uncertainties are reported in column 8 ($\text{ALT-TG}^{\text{OST}}$) of Table 2.

[41] Since AVISO satellite altimetry data are used in our analysis and *Ostanciaux et al*. [2012], any differences between the two classical altimeter-gauge solutions will be due to be explained from the tide gauge records. In Figure 4, the length differences between the monthly tide gauge time series used in this study and the annual tide gauge time series used by *Ostanciaux et al*. [2012] clearly contribute to the disagreement at tide gauges in Whangarei, Auckland, and Lyttelton (Table 2). Moreover, both studies report unrealistic estimates of 4.28 mm/yr and 8.29 mm/yr at the tide gauge in New Plymouth, which could be due to gauge malfunction through the altimetry data period (see http://www.psmsl.org/data/obtaining/stations/996.php). For this reason, the altimeter-gauge vertical land motion is not considered even though its effect is tested during the implementation of the advanced approach.

[42] The advanced altimeter-gauge approach yields uncertainties between 0.2 mm/yr and 0.7 mm/yr, with a mean uncertainty of 0.4 mm/yr compared to 0.7 mm/yr of the classical approach, which is in agreement with *Kuo et al*. [2008] and *Wöppelmann and Marcos* [2012]. Vertical land motion estimates are also significantly modified with differences larger than 2 mm/yr at tide gauges in Timaru and Bluff (Table 2).

[43] The robustness of the advanced altimeter-gauge approach is assessed in four steps. First, as mentioned in section 3.2.1, we investigate the sensitivity of both approaches to the altimetric time series of the closest grid point or the average within a radius of 1/2° around the tide gauge sites. The differences in the vertical land motion estimates are within one-sigma level and do not exceed 0.2 mm/yr in the case of the classical approach and are insignificantly different from zero in the advanced approach.

[44] In the second step, we examine the effect of removing one tide gauge, consecutively different, from the set of tide gauges with discontinuous sea level records (i.e., Whangarei, Moturiki, New Plymouth, Nelson, Timaru, and Bluff). The effects on vertical land motion rates are smaller than ∼0.1–0.2 mm/yr, except when the New Plymouth tide gauge is removed. In that case, rate estimates of the other sites decrease by 0.43 mm/yr, although the resultant rate at New Plymouth of 0.21 ± 0.40 mm/yr (not shown in Table 2) is consistent with both geological and GPS estimates (Table 2). The reason for this particular sensitivity to the New Plymouth site is related to the unrealistically high input rate of 4.28 mm/yr derived from the classical approach (Table 2). It is worth mentioning that *Wöppelmann and Marcos* [2012] find similar impact value (0.4 mm/yr) along the Atlantic Iberian coast when including one specific tide gauge (Cascais) exhibiting unrealistic uplift with no reported explanation. Assuming New Plymouth input rate varies between ±2 mm/yr, which is four times the GPS (-0.47 ± 0.28) and geological (0.5 ± 0.5 mm/yr) estimates (Table 2), the effect is reduced to 0.2 mm/yr.

[45] In the third step, the analysis period is restricted to (1950–2011) interval as it corresponds to a temporally homogeneous data set of the tide gauges used in this study (Figure 2). In this case, the vertical land motion estimates change about ±0.20 mm/yr at all tide gauge sites, whereas the uncertainties increase by +0.10 mm/yr at Auckland, Wellington, Lyttelton, and Dunedin only.

[46] In the last step, where we use only the four tide gauges with long-term continuous records at Auckland, Wellington, Lyttelton, and Dunedin, the effect on the vertical land motion rates is smaller than 0.07 mm/yr compared to the case involving the total set of sites without including the New Plymouth tide gauge. According to the foregoing considerations, estimates at the New Plymouth tide gauge using both altimeter-gauge approaches have been discarded.

[47] In the case of a separate treatment of the three regions of New Zealand (i.e., the removal of the link in scheme (4)), the effects on vertical land motions at tide gauges sites of the South and North Islands are smaller than −0.22 mm/yr and −0.01 mm/yr, respectively, whereas the two tide gauge sites at Cook Strait, poorly linked by one constraint equation only (one pair of tide gauges: Wellington and Nelson after New Plymouth removal), show relatively higher sensitivity and a change of estimated rate of +0.51 mm/yr.

4.3. Vertical Land Motion Estimates Comparison

[48] Figure 5 illustrates the comparison between geological vertical land motion estimates and those derived from GPS (the combined ULR5 and NZ3P solution) or the advanced altimeter-gauge approach. It is clear that GPS performs poorly relative to geology with mean site biases of 1.0 mm/yr, whereas strong agreement is found between the advanced altimeter-gauge and the geology estimates (Figure 5). All tide gauge sites show negligible differences between the geology and the advanced altimeter-gauge solutions. While estimates at four tide gauge sites in Moturiki, Nelson, Lyttelton, and Dunedin display a relative positive mean site bias of 0.22 mm/yr, an equivalent but negative relative mean site bias of −0.29 mm/yr is displayed at four other tide gauge sites in Whangarei, Auckland, Wellington, and Bluff. Moreover, both solutions show identical vertical rates at the Timaru tide gauge site.

[49] Slow slip events may result in potential biases that may explain the spurious signals affecting the vertical time series of the cGPS stations located around the Wanganui

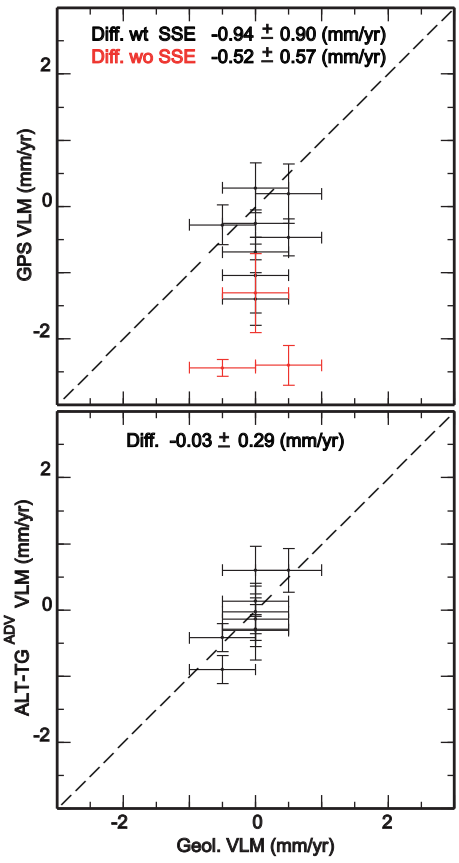

Figure 5. Geological vertical land motions against (top) GPS mean vertical land motions (MVLM) and (bottom) advanced altimeter-gauge vertical land motions (estimates and uncertainties are given in Table 2). Vertical rate differences and uncertainties between GPS (including and not including cGPS affected by slow slip events), advanced altimeter-gauge, and geological estimates are also given.

basin (GLDB, NLSN, WGTN, and WGTT in Figures 1 and 3). Slow slip events occur on the subduction interface that underlies this region and have been recorded since the installation of cGPS stations in the region [e.g., *Wallace and Beavan*, 2010; *Wallace et al.*, 2012]. These slow earthquake-like events, both beneath and offshore in this region, have durations of a year or more and recurrence intervals on the order of 3 years (Figure 3). Consequently, the vertical time series at these four cGPS sites give higher subsidence rates compared to the geology and the advanced altimeter-gauge estimates with mean site biases of −2.05 mm/yr and −1.73 mm/yr, respectively. These time series need to be sufficiently long so that the estimated trend is not significantly affected by the slow slip events and hence do not bias the vertical land motion rates. It is worth mentioning that possible variations in rates of subsidence have not been addressed. Although not detected, it should also be noted that slow slip events may affect also the tide gauge sea level records of Wellington (110 years) and Nelson (55 years), but the effect will average and hence vanishes when deriving sea level trend or introducing the constraint equations from long-term sea level time series (Figure 2).

[50] In regions farther from slow slip events, GPS vertical land motions show negative biases relative to the geology and the advanced altimeter-gauge estimates at all cGPS stations except at BLUF and LYTT (Table 2 and Figure 5). Indeed, the cGPS site at WAIM shows statistically significant difference of −1.40 mm/yr relative to the geology and the advanced altimeter-gauge estimates. The main limitation that may explain this disagreement is that the actual tide gauge benchmark at Timaru and the cGPS antenna at WAIM are distant by 39 km (Table 2). In addition, the cGPS stations at WHNG, TRNG, NPLY, DUNT, and OUSD display negative mean site biases of −0.75 mm/yr and −0.66 mm/yr relative to the geology and the advanced altimeter-gauge estimates, respectively (Table 2 and Figure 5). In contrast, cGPS sites at BLUF and LYTT also exhibit small positive mean site biases of 0.25 mm/yr and 0.36 mm/yr. This good agreement further suggests that the earthquakes affecting Bluff and Lyttelton (Figure 3 and Table 2) are unlikely to have biased the derived vertical land motion estimates. Furthermore, the cGPS sites at AUCK, TAKL, and LYTT show very slow subsidence that absolutely agrees with the geology and the advanced altimeter-gauge estimates, with a zero mean site bias.

[51] Finally, the geological and GPS vertical land motions at the four salt-marsh sites are completely consistent with trend differences of $<\pm 0.3$ mm/yr, except at the Whanganui Inlet site where the GPS vertical time series at GLDB seems to be strongly affected by slow slip events (Figure 3).

4.4. Sea Level Change Around New Zealand

4.4.1. Instrumental Absolute Sea Level Rise

[52] To further evaluate the performance of the three various vertical land motion techniques (Table 2), the tide gauge absolute sea level trends, deduced using geology, GPS, and advanced altimeter-gauge rates are summarized in Table 3 and illustrated in Figure 6.

[53] When the advanced altimeter-gauge approach is used to eliminate vertical land motion from tide gauge relative sea level trends (Figure 6a), the dispersion among absolute sea level rise rates is clearly diminished (Figure 6c) as expected from the inherent assumption introduced in equation (2). Interestingly, when geological vertical rates are used instead, a similar absolute sea level pattern is also results (Figure 6d).

[54] The four absolute sea level curves of Auckland, Wellington, Lyttelton, and Dunedin are inferred from relative sea level trends computed for the different time periods shown in Table 3 and corrected for vertical land motion using the geology and the advanced altimeter-gauge solutions (Figures 6c and 6d). These curves show a good agreement, except at the last period from 1975 to 2011, where the Lyttelton curve (in blue) shows lower sea level rise (Figures 6c and 6d). According to an unpublished LINZ documentation, a new metric tide pole was installed at Lyttelton tide gauge in 1980, and the datum was adjusted according to leveling measurements. Therefore, this equipment change and the correction applied to the mean sea level data at this tide gauge may have affected its relative sea level trend for this period.

Table 3. Rates of Relative Sea Level Change at Tide Gauges and Salt-Marsh Sites Derived From (i) Geological, GPS, and Advanced Altimeter-Gauge (ALT-TG^{ADV}) Vertical Land Motion Estimates at Tide Gauges Sites and From (ii) Geological and GPS Vertical Land Motion Estimates at Salt-Marsh Sites[a]

				Absolute Sea Level Change		
Site	Data	RSL Source	Period	Geol. (mm/yr)	GPS (mm/yr)	ALT-TG^{ADV} (mm/yr)
Whangarei	TG	HB12	1962–	2.20 ± 0.78	1.16 ± 0.83	1.82 ± 0.86
	TG	This study	1975–	2.72 ± 0.82	1.68 ± 0.86	2.47 ± 0.82
Auckland	TG	HB12	1899–	1.70 ± 0.52	1.44 ± 0.25	1.54 ± 0.34
	TG	This study	1899–	1.51 ± 0.51	1.25 ± 0.23	1.44 ± 0.40
Puhinui	SM	GR12	1900–	3.00 ± 0.71	2.86 ± 0.63	–
Moturiki	TG	HB12	1951–	2.40 ± 0.54	2.09 ± 0.49	2.49 ± 0.54
	TG	This study	1974–	2.35 ± 0.68	2.04 ± 0.64	2.39 ± 0.54
N. Plymouth	TG	HB12	1920–	2.00 ± 0.54	1.03 ± 0.34	–
	TG	This study	1920–	1.87 ± 0.67	0.90 ± 0.52	–
Whanganui	SM	FI12	1900–	4.00 ± 0.71	1.10 ± 0.58	–
Nelson	TG	HB12	1941–	1.30 ± 0.56	−0.01 ± 0.65	1.98 ± 0.59
	TG	This study	1956–	0.59 ± 0.61	−0.72 ± 0.69	1.28 ± 0.59
Wellington	TG	HB12	1901–	1.70 ± 0.52	−0.24 ± 0.18	1.28 ± 0.33
	TG	This study	1901–	1.82 ± 0.51	−0.12 ± 0.17	1.38 ± 0.34
Lyttelton	TG	HB12	1901–	1.50 ± 0.52	1.72 ± 0.34	1.56 ± 0.34
	TG	This study	1901–	1.40 ± 0.51	1.62 ± 0.32	1.41 ± 0.34
Timaru	TG	HB12	1936–	1.70 ± 0.56	0.30 ± 0.47	1.65 ± 0.73
	TG	This study	1963–	2.24 ± 0.79	0.84 ± 0.73	2.15 ± 1.13
Dunedin	TG	HB12	1899–	1.30 ± 0.52	0.61 ± 0.19	1.46 ± 0.36
	TG	This study	1899–	1.28 ± 0.51	0.59 ± 0.16	1.51 ± 0.36
Pounawea	SM	GE08	1900–	2.80 ± 0.71	3.08 ± 0.63	–
Waikawa	SM	FI12	1900–	3.30 ± 0.71	3.58 ± 0.63	–
Bluff	TG	HB12	1926–	1.80 ± 0.52	2.08 ± 0.41	1.47 ± 0.36
	TG	This study	1923–	1.85 ± 0.54	2.13 ± 0.43	1.57 ± 0.39

[a]The uncertainties are obtained by propagating the formal uncertainties of relative sea level and vertical land motion variables assuming zero correlation. FI12, GE08, GR12, and HB12 denote the works of *Figueira* [2012], *Gehrels et al*. [2008], *Grenfell et al*. [2012], and *Hannah and Bell* [2012].

[55] The relative sea level trend at Moturiki tide gauge reported by *Hannah and Bell* [2012] for the period (1951–2008) cannot be realistic since it cannot be fitted within the four absolute sea level curves drawn with respect to the geology and the advanced altimeter-gauge approach vertical land motion estimates (Table 1, and Figures 6c and 6d). Furthermore, both absolute sea level trends at Nelson tide gauge cannot be fitted within the four curves using geological vertical land motion estimates (Figure 6d), which may suggest that Nelson is geologically uplifting by ∼0.5–1.0 mm/yr rather than stable as compiled by *Beavan and Litchfield* [2012] in Table 2.

[56] Moreover, Figures 6c and 6d reveal that three well-defined phases in terms of absolute sea level change can be distinguished from these curves with respect to the geology and the advanced altimeter-gauge solutions (Figure 6e). On average, the first phase (1900–1936) is marked by an increase of absolute sea level rise from 1.46 ± 0.10 mm/yr to 1.72 ± 0.10 mm/yr, followed in the second phase (1936–1956) by a decrease to 1.48 ± 0.09 mm/yr, and then a substantial increase to 2.60 ± 0.10 mm/yr during the third phase (1956–1975).

[57] Most striking is that none of all these common features between the geology and the advanced altimeter-gauge solutions can be seen from the absolute sea level rates inferred using GPS estimates (Figure 6b). This is partly due to the inherent biases (up to −2.05 mm/yr in the case of slow slip events) affecting the GPS solution that are of the same order of magnitude as the expected 20th century sea level rise rate of 1.7 mm/yr [e.g., *Holgate*, 2007; *Church and White*, 2011]. The sole outcome from GPS solution (Figure 6b) is the consistency between the 20th sea level rise trends of Auckland (North Island) and Lyttelton (South Island) averaged at 1.51 ± 0.18 mm/yr that is in agreement with sea level change rate derived with respect to the advanced altimeter-gauge approach and the geology vertical estimates. Actually, it confirms our combined treatment of scheme (4) and the uniformity of the 20th century sea level rise along the coast of New Zealand.

4.4.2. Instrumental and Proxy Absolute Sea Level Rise Comparison

[58] To assess to what extent the vertical land motion could account for the observed dispersion and spatial variability in proxy and instrumental relative sea level trends along the New Zealand coast (Table 1), absolute sea level rates at tide gauge and salt-marsh sites are computed using the three vertical land motion solutions, and are spatially illustrated in Figure 7.

[59] The consistency of the geology and the advanced altimeter-gauge solutions and their overall disagreement with GPS solution are being reflected on the absolute sea level rates at tide gauge sites (Figures 5 and 7). Absolute sea level rates at tide gauge sites inferred from the geology and the advanced altimeter-gauge estimates show a definite

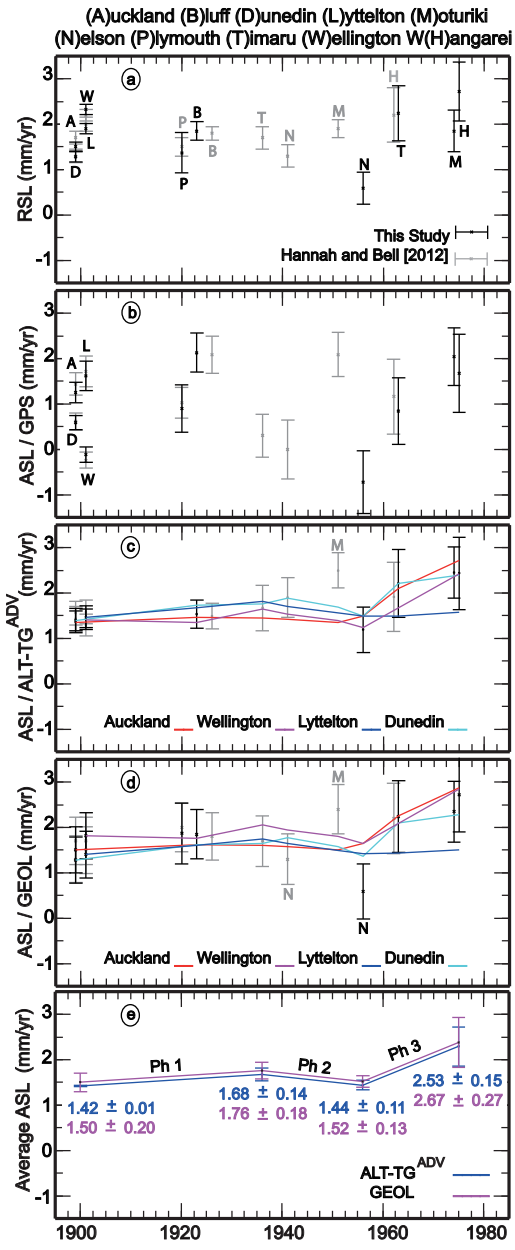

Figure 6. Rates of sea level change and uncertainties along New Zealand coasts: (a) relative sea level trends from tide gauges as computed by *Hannah and Bell* [2012] (in gray) and this study (in black), and absolute sea level (ASL) trends using (b) GPS, (c) advanced altimeter-gauge, and (d) geological vertical land motions estimates. Also shown are absolute sea level rate time series of Auckland (in red), Wellington (in pink), Lyttelton (in blue), and Dunedin (in cyan), as deduced from relative sea level trends computed at all epochs given in Table 3 and corrected using the advanced altimeter-gauge approach and the geological vertical land motion estimates. (e) Three distinguished phases in terms of absolute sea level change extracted from the advanced altimeter-gauge approach (in blue) and the geology (in pink).

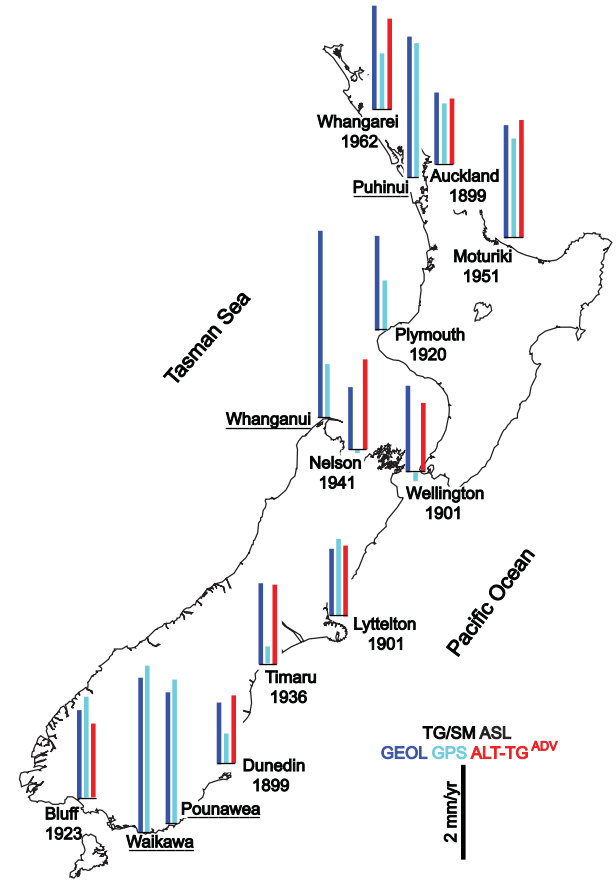

Figure 7. Rates of sea level change at tide gauge and salt-marsh (underlined names) sites corrected for vertical land motion using geological (blue), GPS (cyan), and advanced altimeter-gauge (red) solutions (Table 3). ASL, TG, and SM, respectively, stand for Absolute Sea Level, Tide Gauge, and Salt-Marsh.

agreement and larger values compared to those inferred from GPS except at Bluff and Lyttelton sites. In addition, slow slip events affecting time series of cGPS stations of WGTN and NLSN lead also to smaller and spurious absolute sea level rates at the Wellington and Nelson tide gauges (Figures 3 and 7).

[60] As result of vertical land motion agreement at Puhinui, Pounawea, and Waikawa Harbour, absolute sea level rates inferred from GPS and geology solutions at these salt-marsh sites agree. However, a disagreement is found at Whanganui Inlet site where slow slip events affecting the GLDB time series also lead to a lower absolute sea level rate (Figure 7). The proxy absolute sea level displays twice the 20th century instrumental estimates with average rates of 3.28 ± 0.45 mm/yr and 3.17 ± 0.30 mm/yr with respect to geology and GPS solutions (Table 3). At this stage, it is clear that vertical land motion is not responsible for the high sea level change estimates reported in New Zealand salt-marsh sea level reconstructions [*Gehrels et al.*, 2008, 2012; *Figueira*, 2012; *Grenfell et al.*, 2012].

[61] *Brain et al.* [2012] have explored the contribution of sediment compression, a key compaction process, to the magnitude of recent accelerated sea level rise reconstructed from salt-marsh sediments. The authors find that compression can be a significant contributor and the magnitude of its effect can be sufficient to add ~0.1–0.4 mm/yr to local

sea level rise. However, they conclude that for an improved understanding of all the processes leading to compaction [e.g., biodegradation] collection of new data are required to draw a firm conclusion about the magnitude of the effect of compaction in highly organic sediments [*Brain et al*., 2012].

4.5. Regional Absolute Sea Level Change

[62] To assess the regional variability of the 20th century sea level rise, Figure 8 illustrates a comparison between the New Zealand rate of 1.46 ± 0.10 mm/yr with estimates from Australia, Tasmania, and Macquarie Island as reported from previous sea level studies.

[63] *Burgette et al*. [2013] find an average rate of sea level rise around Australia since 1900 to be 1.40 ± 0.60 mm/yr for the network of 43 tide gauges including the two longest records from Sydney and Fremantle tide gauges (Figure 8). Their investigation reveals a spatially coherent pattern of sea level rise around Australia coastline, with the highest rates ∼3–5 mm/yr occurring in the north and the lowest rates ∼0–2 mm/yr along the southern coast.

[64] Observations of sea level at Port Arthur (Tasmania, Figure 8) based on a 2 year record made in 1841–1842, a 3 year record made in 1999–2002, and intermediate observations made in 1875–1905, 1888, and 1972, indicate an average absolute rate of sea level rise of 1.00 ± 0.30 mm/yr over the whole period (1841–2002), once geological land uplift has been eliminated [*Hunter et al*., 2003]. If it is assumed that most of this sea level rise occurred since about 1890, then the corresponding estimate of rise (1890–2002) becomes 1.40 ± 0.30 mm/yr [*Hunter et al*., 2003].

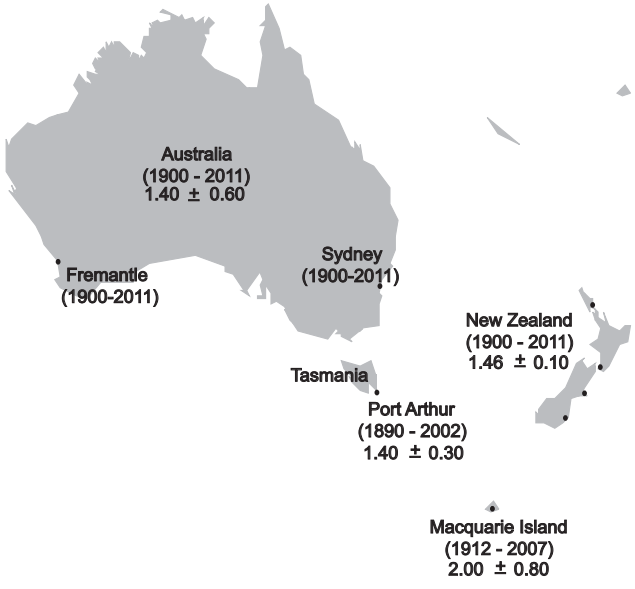

Figure 8. Map represents regional absolute sea level rise (in mm/yr) as estimated in this study along New Zealand coast, and from other completed sea level studies that involve Australia long-term recording tide gauges (Fremantle and Sydney) [*Burgette et al*., 2013] and historical tide gauge observations at Macquarie Island [*Watson et al*., 2010], and Tasmania (Port Arthur) [*Hunter et al*., 2003].

[65] *Watson et al*. [2010] combine nine months of sea level data from (1912–1913) with intermediate observations in (1969–1971), 1982, and (1998–2007) to estimate absolute sea level rise in Macquarie Island at 2.00 ± 0.80 mm/yr once ongoing subsidence of this Island has been constrained by the GPS estimate of vertical velocity of -2.46 ± 0.64 mm/yr (Figure 8).

[66] Based on the reported 20th century sea level rise rates from southern Australia [*Burgette et al*., 2013], Port Arthur [*Hunter et al*., 2003], and New Zealand, the spatial variability is likely to be insignificant within uncertainties, with estimates of regional rates of 1.40 mm/yr. However, accurate knowledge on vertical land motions is needed for robust sea level rise projections. Therefore, no firm conclusion can be drawn about this rate since sea level rise rates from Australia and Port Arthur are corrected using cGPS stations within 100 km of a tide gauge [*Burgette et al*., 2013] and geological evidences [*Hunter et al*., 2003], respectively.

5. Conclusion

[67] This paper investigates the complexity of studying absolute sea level rise in regions that straddle New Zealand's deforming plate boundary where earthquakes and slow slip events can contribute to the vertical land motion at tide gauge and salt-marsh sites.

[68] A highly coherent absolute sea level rise pattern is inferred once relative sea level trends from tide gauges are corrected using the geology and the advanced altimeter-gauge vertical land motion estimates. New Zealand 20th century absolute sea level change is estimated at 1.46 ± 0.10 mm/yr that is consistent with previous sea level studies from Australia and Tasmania, and in agreement with the global sea level rise of 1.7 ± 0.20 mm/yr. The surprising outcome is the failure to infer any clear time-varying pattern of sea level rise when correcting tide gauge sea level records for vertical land motion with GPS data.

[69] In contrast, New Zealand's 20th century proxy records display high absolute sea level rates averaged at 3.23 ± 0.27 mm/yr once GPS and geological vertical land motion corrections are applied at the salt-marsh sites. The role of autocompaction in salt-marsh sequences plays may only explain some of the differences from rates calculated from instrumental data but it is currently poorly constrained and needs further investigation. Similarly, the results as derived from transfer functions can contribute significant errors and online access to raw data and details of the transfer function calculations used would help with validation.

[70] **Acknowledgments.** We thank CalTech/JPL for providing the GIPSY-OASIS II. We acknowledge the New Zealand GeoNet project and its sponsors EQC, GNS Science, and LINZ, for providing raw GPS data used in this study. Tide gauge data are from LINZ, NIWA, PSMSL, and UHSLC. Altimetry data and DAC products are obtained from AVISO, with support from CNES. The SONEL data assembly center is also acknowledged for providing a comprehensive access to GPS vertical velocity solution at tide gauges. Figures were produced using Generic Mapping Tools [*Wessel and Smith*, 1995]. We would like to thank Matt King, Paul Tregoning, and two other anonymous reviewers for their extensive and constructive comments. We would like also to thank Anny Cazenave for fruitful discussions. This paper is IPGP contribution number 3447.

References

Altamimi, Z., X. Collilieux, and L. Metivier (2011), ITRF2008: An improved solution of the international terrestrial reference frame, *J. Geod.*, *85*(5), 457–473, doi:10.1007/s00190-011-0444-4.

Argus, D. F., M. B. Heflin, G. Peltzer, F. Crampé, and F. H. Webb (2005), Interseismic strain accumulation and anthropogenic motion in metropolitan Los Angeles, *J. Geophys. Res.*, *110*, B04401, doi:10.1029/2003JB002934.

Bar-Sever, Y. E., P. M. Kroger, and J. A. Borjesson (1998), Estimating horizontal gradients of tropospheric path delay with a single GPS receiver, *J. Geophys. Res.*, *103*(B3), 5019–5035, doi:10.1029/97JB03534.

Beavan, J., and N. J. Litchfield (2012), Vertical land movement around the New Zealand Coastline: Implications for sea-level rise, *GNS Sci. Rep. 2012/29*, 41 pp , GNS Science, Lower Hutt, New Zealand.

Bertiger, W., S. Desai, B. Haines, N. Harvey, A. Moore, S. Owen, and J. Weiss (2010), Single receiver phase ambiguity resolution with GPS data, *J. Geod.*, *84*(5), 327–337, doi:10.1007/s00190-010-0371-9.

Boehm, J., B. Werl, and H. Schuh (2006), Troposphere mapping functions for GPS and very long baseline interferometry from European Centre for Medium-Range Weather Forecasts operational analysis data, *J. Geophys. Res.*, *111*, B02406, doi:10.1029/2005JB003629.

Brain, M. J., A. J. Long, D. N. Petley, B. P. Horton, and R. J. Allison (2011), Compression behaviour of minerogenic low energy intertidal sediments, *Sediment. Geol.*, *233*, 28–41, doi:10.1016/j.sedgeo.2010.10.005.

Brain, M. J., A. J. Long, S. A. Woodroffe, D. N. Petley, D. G. Milledge, and A. C. Parnell (2012), Modelling the effects of sediment compaction on salt marsh reconstructions of recent sea-level rise, *Earth Planet. Sci. Lett.*, *345–348*, 180–193, doi:10.1016/j.epsl.2012.06.045.

Burgette, R., C. Watson, J. Church, N. White, P. Tregoning, and R. Coleman (2013), Characterizing and minimizing the effects of noise in tide gauge time series: Relative and geocentric sea level rise around Australia, *Geophys. J. Int.*, *194*(2), 719–736, doi:10.1093/gji/ggt131.

Carrere, L., and F. Lyard (2003), Modeling the barotropic response of the global ocean to atmospheric wind and pressure forcing—Comparisons with observations, *Geophys. Res. Lett.*, *30*(6), 1275, doi:10.1029/2002GL016473.

Chinn, T. J., C. Heydenrych, and M. J. Salinger (2005), Use of ELA as a practical method of monitoring glacier response to climate in New Zealand's Southern Alps, *J. Glaciol.*, *51*(172), 85–95, doi:10.3189/172756505781829593.

Church, J. A., and N. J. White (2011), Sea-level rise from the late 19th to the early 21st Century, *Surv. Geophys.*, *32*, 585–602, doi:10.1007/s10712-011-9119-1.

DeMets, C., R. G. Gordon, and D. F. Argus (2010), Geologically current plate motions, *Geophys. J. Int.*, *181*(1), 1–80, doi:10.1111/j.1365-246X.2009.04491.x.

Edwards, R. J., O. V. D. Plassche, W. R. Gehrels, and A. J. Wright (2004), Assessing sea-level data from Connecticut, USA, using a foraminiferal transfer function for tide levels, *Mar. Micropaleontol.*, *51*, 239–255.

Figueira, B. O. (2012), Salt marsh foraminiferal proxy record of late Holocene sea-level rise, South Island, New Zealand, PhD thesis, 199 pp., Univ. of Auckland, Auckland, New Zealand.

Gehrels, R. W., J. R. Kirby, A. Prokoph, R. M. Newnham, E. P. Achterberg, H. Evans, S. Black, and D. B. Scott (2005), Onset of recent rapid sea-level rise in the western Atlantic Ocean, *Quat. Sci. Rev.*, *24*, 2083–2100.

Gehrels, W. R., B. W. Hayward, R. M. Newnham, and K. E. Southall (2008), A 20th century acceleration of sea-level rise in New Zealand, *Geophys. Res. Lett.*, *35*, L02717, doi:10.1029/2007GL032632.

Gehrels, W. R., S. L. Callard, P. T. Moss, W. A. Marshall, M. Blaauw, J. Hunter, J. A. Milton, and M. H. Garnett (2012), Nineteenth and twentieth century sea-level changes in Tasmania and New Zealand, *Earth Planet. Sci. Lett.*, *315–316*, 94–102, doi:10.1016/j.epsl.2011.08.046.

Grenfell, H. R., B. W. Hayward, R. Nomura, and A. T. Sabaa (2012), A foraminiferal proxy record of 20th century sea-level rise in the Manukau Harbour, New Zealand, *Mar. Freshwater Res.*, *63*, 370, doi:10.1071/MF11208.

Hannah, J. (1990), Analysis of mean sea level data from New Zealand for the period 1899–1988, *J. Geophys. Res.*, *95*(B8), 12,399–12,405, doi:10.1029/JB095iB08p12399.

Hannah, J. (2004), An updated analysis of long-term sea level change in New Zealand, *Geophys. Res. Lett.*, *31*, L03307, doi:10.1029/2003GL019166.

Hannah, J., and R. G. Bell (2012), Regional sea level trends in New Zealand, *J. Geophys. Res.*, *117*, C01004, doi:10.1029/2011JC007591.

Hayward, B. W., H. R. Grenfell, H. R., and D. B. Scott (1999), Tidal range of marsh foraminifera for determining former sea-level heights in New Zealand, *N. Z. J. Geol. Geophys.*, *42*, 395–413.

Herring, T. A. (2003), Matlab Tools for viewing GPS velocities and time series, *GPS Solut.*, *7*(3), 194–199, doi:10.1007/s10291-003-0068-0.

Holgate, S. J. (2007), On the decadal rates of sea level change during the twentieth century, *Geophys. Res. Lett.*, *34*, L01602, doi:10.1029/2006GL028492.

Hunter, J., R. Coleman, and D. Pugh (2003), The Sea Level at Port Arthur, Tasmania, from 1841 to the Present, *Geophys. Res. Lett.*, *30*, 1401, doi:10.1029/2002GL016813.

IERS Conventions (2010), ERS Tech. Note 36, edited by G. Petit and B. Luzum, 179 pp., Bundesamts für Kartogr. und Geod., Frankfurt am Main, Germany.

Kemp, A. C., B. P. Horton, D. R. Corbett, S. J. Culver, R. J. Edwards, and V. D. O. Plassche (2009), The relative utility of foraminifera and diatoms for reconstructing late Holocene sea-level change in North Carolina, USA, *Quat. Res.*, *71*, 9–21.

King, M. A., M. Keshin, P. L. Whitehouse, I. D. Thomas, G. Milne, and R. E. M. Riva (2012), Regional biases in absolute sea-level estimates from tide gauge data due to residual unmodeled vertical land movement, *Geophys. Res. Lett.*, *39*, L14604, doi:10.1029/2012GL052348.

Kuo, C. Y., C. K. Shum, A. Braun, and J. X. Mitrovica (2004), Vertical crustal motion determined by satellite altimetry and tide gauge data in Fennoscandia, *Geophys. Res. Lett.*, *31*, L01608, doi:10.1029/2003GL019106.

Kuo, C. Y., C. K. Shum, A. Braun, K. C. Cheng, and Y. Yi (2008), Vertical motion determined using satellite altimetry and tide gauges, *Terr. Atmos. Oceanic Sci.*, *19*, 21–35, doi:10.3319/TAO.2008.19.1–2.21(SA).

Langbein, J. (2012), Estimating rate uncertainty with maximum likelihood: Differences between power-law and flicker-random-walk models, *J. Geod.*, *86*(9), 775–783, doi:10.1007/s00190-012-0556-5.

Langbein, J., and H. Johnson (1997), Correlated errors in geodetic time series: Implications for time-dependent deformation, *J. Geophys. Res.*, *102*(B1), 591–603, doi:10.1029/96JB02945.

Lemoine, F. G., et al. (2010), Towards development of a consistent orbit series for TOPEX, Jason-1, and Jason-2, *Adv. Space Res.*, *46*(12), 1513–1540, doi:10.1016/j.asr.2010.05.007.

Leorri, E., B. P. Horton, and A. Cearreta (2008), Development of a foraminifera-based transfer function in the Basque marshes, N. Spain: Implications for sea-level studies in the Bay of Biscay, *Mar. Geol.*, *251*, 60–74.

Lyard, F., F. Lefevre, T. Letellier, and O. Francis (2006), Modelling the global ocean tides: Modern insights from FES2004, *Ocean Dyn.*, *56*, 394–415.

Mao, A., C. G. A. Harrison, and T. H. Dixon (1999), Noise in GPS coordinate time series, *J. Geophys. Res.*, *104*(B2), 2797–2816, doi:10.1029/1998JB900033.

Massey, A. C., W. R. Gehrels, D. J. Charman, and S. J. White (2006), An intertidal foraminifera-based transfer function for reconstructing Holocene sea-level change in southwest England, *J. Foraminiferal Res.*, *36*, 215–232.

Mazzotti, S., C. Jones, and R. E. Thomson (2008), Relative and absolute sea level rise in western Canada and northwestern United States from a combined tide gauge-GPS analysis, *J. Geophys. Res.*, *113*, C11019, doi:10.1029/2008JC004835.

Menke, W. (2012), *Geophysical Data Analysis: Discrete Inverse Theory*, 3rd ed., Matlab ed., 330 pp., Academic Press, San Diego, Calif.

Mitchum, G. T. (1998), Monitoring the stability of satellite altimeters with tide gauges, *J. Atmos. Oceanic Technol.*, *15*(3), 721–730, doi:10.1175/1520–0426(1998)015<0721:MTSOSA>2.0.CO;2.

Ostanciaux, E., L. Husson, G. Choblet, C. Robin, and K. Pedoja (2012), Present-day trends of vertical ground motion along the coast lines, *Earth Sci. Rev.*, *110*(1–4), 74–92, doi:10.1016/j.earscirev.2011.10.004.

Peltier, W. R. (2004), Global glacial isostasy and the surface of the ice-age earth: The ICE-5G (VM2) model and GRACE, *Annu. Rev. Earth Planet. Sci.*, *32*, 111–149, doi:10.1146/annurev.earth.32.082503.144359.

Ponte, R. M., and R. D. Ray (2002), Atmospheric pressure corrections in geodesy and oceanography: A strategy for handling air tides, *Geophys. Res. Lett.*, *29*(24), 2153, doi:10.1029/2002GL016340.

Ray, R. D., B. D. Beckley, and F. G. Lemoine (2010), Vertical crustal motion derived from satellite altimetry and tide gauges, and comparisons

with DORIS, *Adv. Space Res.*, *45*(12), 1510–1522, doi:10.1016/j.asr.2010.02.020.

Santamaria-Gomez, A., M. Gravelle, X. Collilieux, M. Guichard, B. Martín Míguez, P. Tiphaneau, and G. Wöppelmann (2012), Mitigating the effects of vertical land motion in tide gauge records using a state-of-the-art GPS velocity field, *Global Planet. Change*, *98–99*, 6–17, doi:10.1016/j.gloplacha.2012.07.007.

Schmid, R., P. Steigenberger, G. Gendt, M. Ge, and M. Rothacher (2007), Generation of a consistent absolute phase center correction model for GPS receiver and satellite antennas, *J. Geod.*, *81*(12), 781–798, doi:10.1007/s00190-007-0148-y.

Scott, D. B., C. T. Schaefer, and F. S. Medioli (2001), *Monitoring in Coastal Environments Using Foraminifera and Thecamoebian Indicators*, Cambridge Univ. Press, Cambridge, U. K.

Southall, K. E., W. R. Gehrels, and B. W. Hayward (2006), Foraminifera in a New Zealand salt marsh and their suitability as sea-level indicators, *Mar. Micropaleontol.*, *60*, 167–179, doi:10.1016/j.marmicro.2006.04.005.

Tregoning, P., and T. A. Herring (2006), Impact of a priori zenith hydrostatic delay errors on GPS estimates of station heights and zenith total delays, *Geophys. Res. Lett.*, *33*, L23303, doi:10.1029/2006GL027706.

Tregoning, P., and C. Watson (2009), Atmospheric effects and spurious signals in GPS analyses, *J. Geophys. Res.*, *114*, B09403, doi:10.1029/2009JB006344.

Tregoning, P., and C. Watson (2011), Correction to Atmospheric effects and spurious signals in GPS analyses, *J. Geophys. Res.*, *116*, B02412, doi:10.1029/2010JB008157.

Trupin, A., and J. Wahr (1990), Spectroscopic analysis of global tide gauge sea level data, *Geophys. J. Int.*, *100*, 441–453, doi:10.1111/j.1365-246X.1990.tb00697.x.

Volkov, D. L., G. Larnicol, and J. Dorandeu (2007), Improving the quality of satellite altimetry data over continental shelves, *J. Geophys. Res.*, *112*, C06020, doi:10.1029/2006JC003765.

Walcott, R. I. (1984), The kinematics of the plate boundary zone through New Zealand: A comparison of short- and long-term deformations, *Geophys. J. R. Astron. Soc.*, *79*, 613–633, doi:10.1111/j.1365-246X.1984.tb02244.x.

Wallace, L. M., and J. Beavan (2010), Diverse slow slip behavior at the Hikurangi subduction margin, New Zealand, *J. Geophys. Res.*, *115*, B12402, doi:10.1029/2010JB007717.

Wallace, L. M., J. Beavan, S. Bannister, and C. Williams (2012), Simultaneous long-term and short-term slow slip events at the Hikurangi subduction margin, New Zealand: Implications for processes that control slow slip event occurrence, duration, and migration, *J. Geophys. Res.*, *117*, B11402, doi:10.1029/2012JB009489.

Watson, C., R. Burgette, P. Tregoning, N. White, J. Hunter, R. Coleman, R. Handsworth, and H. Brolsma (2010), Twentieth century constraints on sea level change and earthquake deformation at Macquarie Island, *Geophys. J. Int.*, *182*, 781–796, doi:10.1111/j.1365-246X.2010.04640.x.

Webb, F. H., and J. F. Zumberge (1995), An introduction to GIPSY-OASIS-II precision software from the analysis of data from the Global Positioning System, *Rep. JPL D-11088*, California Institute of Technology, Pasadena, Calif.

Wessel, P., and W. H. F. Smith (1995), New version of generic mapping tools released, *EOS Trans. AGU*, *76*, 329.

Williams, S. D. P. (2008), CATS: GPS coordinate time series analysis software, *GPS Solut.*, *12*(2), 147–153, doi:10.1007/s10291-007rr0086-4.

Woodworth, P. L. (2012), A note on the nodal tide in sea level records, *J. Coastal Res.*, *28*(2). 316–323, doi:10.2112/JCOASTRES-D-11A-00023.1.

Woodworth, P. L., and R. Player (2003), The permanent service for mean sea level: An update to the 21st century, *J. Coastal Res.*, *19*, 287–295.

Wöppelmann, G., and M. Marcos (2012), Coastal sea level rise in southern Europe and the nonclimate contribution of vertical land motion, *J. Geophys. Res.*, *117*, C01007, doi:10.1029/2011JC007469.

Wöppelmann, G., B. Martin Miguez, M. N. Bouin, and Z. Altamimi (2007), Geocentric sea-level trend estimates from GPS analyses at relevant tide gauges world-wide, *Global Planet. Change*, *57*, 396–406, doi:10.1016/j.gloplacha.2007.02.002.

Zumberge, J. F., M. B. Heflin, D. C. Jefferson, M. M. Watkins, and F. H. Webb (1997), Precise point positioning for the efficient and robust analysis of GPS data from large networks, *J. Geophys. Res.*, *102*(B3), 5005–5017, doi:10.1029/96JB03860.